Original Article

Comparing the Performance of Scatter Correction Methods in Cardiac SPECT Imaging with Technetium-99m and Thallium-201 Radioisotopes

Mahsa Noori-Asl, Maryam Eghbal

Department of Physics, Faculty of Science, University of Mohaghegh Ardabili, Ardabil, Iran

Abstract

Purpose: This study aims to evaluate the performance of dual-energy window (DEW) and triple-energy window (TEW) scatter correction methods in cardiac SPECT imaging with technetium-99m (Tc-99m) and thallium-201 (Tl-201) radioisotopes. **Materials and Methods:** The SIMIND Monte Carlo program was used to simulate the imaging system and produce the required projections. Two phantoms, including the simple cardiac phantom and the NCAT phantom, were used to evaluate the scatter correction methods. The simulations were repeated 5 times for each phantom and finally, the mean values obtained from these 5 tests were used in the analysis of the results. **Results:** The obtained results from this study show that in the case of both investigated phantoms, the use of correction methods leads to improve the contrast of the images obtained from Tc-99m and Tl-201 radioisotopes. In the case of the simple cardiac phantom, the use of DEW and TEW correction methods leads to a relative increase in image contrast of about 23.88% and 12.23% for ^{99m}Tc radioisotope and about 29.19% and 20.98% for ^{201}Tl radioisotope, respectively. This relative increase in the case of the NCAT phantom is about 22.48% and 19.43% for ^{99m}Tc radioisotope and about 27.74% and 24.74% for ^{201}Tl radioisotope, respectively. **Conclusion:** According to the obtained results, despite the higher contrast of the noncorrected images of ^{99m}Tc radioisotope, the relative increase in contrast of the corrected images of ^{201}Tl radioisotope is more than that of ^{99m}Tc radioisotope. Furthermore, for both radioisotopes, the relative increase related to the DEW method is higher than the TEW method.

Keywords: Energy window, image contrast, scatter correction, single-photon emission computed tomography (SPECT), technetium-99m, thallium-201

Received on: 01-03-2024 **Review completed on:** 01-07-2024 **Accepted on:** 01-07-2024 **Published on:** 21-09-2024

Introduction

Thallium-201 (Tl-201) and technetium-99m (Tc-99m) are two commonly used radioisotopes in cardiac SPECT imaging.[1] Tl-201 is generated by a cyclotron and decays to mercury (Hg-201) by electron capture.[2] In this decay, two gamma rays with energies of 135 keV (2.5% abundance) and 167 keV (9.5% abundance) are emitted.[3] The decay product, Hg-201, emits X-rays with an energy range of 68–82 keV (95% abundance).[4] Due to low percentage abundance of both gamma-ray emissions of Tl-201, the Tl-201 imaging rely mostly on the X-ray emissions of Hg-201.[5] The relatively long physical half-life of Tl-201 (73 h) and low-energy X-ray emissions are two important factors that must be considered during imaging. The long half-life necessitates injecting lower doses to minimize radiation exposure. On the other hand, the low-energy emissions lead to longer imaging times and more photon attenuation.[6] Unlike Tl-201, Tc-99m has a physical half-life of 6 h that is short enough to minimize radiation exposure. This radioisotope decays by an isomeric transition involving the gamma-ray emissions with an energy of 140 keV. Compared to the low-energy X-rays used in Tl-201 imaging, these gamma rays have high enough energy to escape the patient's body, resulting in less image attenuation.[7]

Access this article online

Quick Response Code:

Website: www.jmp.org.in

DOI: 10.4103/jmp.jmp_40_24

Address for correspondence: Dr. Mahsa Noori-Asl, Department of Physics, Faculty of Science, University of Mohaghegh Ardabili, Ardabil, Iran.
E-mail: nooriasl.mahsa@gmail.com

How to cite this article: Noori-Asl M, Eghbal M. Comparing the performance of scatter correction methods in cardiac SPECT imaging with technetium-99m and thallium-201 radioisotopes. J Med Phys 2024;49:464-72.

One of the major problems in SPECT imaging is the detection of scattered photons in the main energy window(s) centered about the photopeak(s) of the used radioisotope. Scattering includes two parts: Compton scattering and coherent scattering. In the range of energies considered in nuclear medicine, the probability of Compton scattering is more than that of coherent scattering. Unlike coherent scattering, in Compton scattering, not only the direction of the photon changes, but also the energy of the photon decreases depending on its scattering angle. Due to the limited energy resolution of NaI(Tl) scintillation crystal (about 9%–10% full-width at half-maximum [FWHM] at 140 keV energy), the possibility of detecting a number of scattered photons in the photopeak window is inevitable. Due to the change in the direction of the Compton scattered photons, these photons carry incorrect spatial information. Therefore, the detection of these photons leads to a decrease in image contrast and therefore, a decrease in the quality of the final reconstructed image. Hence, it is necessary to use scatter correction methods to improve image quality and increase diagnostic accuracy.[8]

Many methods for scatter correction of SPECT images have been proposed by different researchers. Among these, two correction methods, the dual-energy window (DEW) method and the triple-energy window (TEW) method, are more widely used due to the simplicity of implementation. The use of these correction methods requires setting one or two additional energy windows in the considered radioisotope spectrum. In the present study, we intend to investigate the performance of these two correction methods in estimating the contribution of scatter counts included in the main energy window used for these two radioisotopes and their efficacy in improving the image quality.

Materials and Methods

In this study, the SIMIND (SIMulation of Imaging Nuclear Detector) Monte Carlo program[9] was used to simulate the SPECT imaging system, define the energy windows required for scatter correction and produce the projections related to each energy window. This program is a simulation code dedicated to SPECT imaging. This simulation code provides separate projections and spectra for the scatter, primary and total counts and is, therefore, a suitable instrument for studying the scattering and evaluating the scatter correction methods.[10] The simulated system consisted of a cylindrical NaI(Tl) scintillation crystal with a radius of 25 cm and a thickness of 1 cm (energy resolution of 10% FWHM and spatial resolution of 0.36 cm at 140 keV), equipped with an aluminum cover with a thickness of 0.2 cm around the crystal and Photo-Multiplier Tubes (PMTs) in the back of the crystal. Furthermore, to restrict the direction of the photons reaching the detector and increase of the image contrast, the front surface of the crystal was equipped with a hexagonal low-energy high-resolution parallel-hole collimator[11] with a hole diameter of 0.18 cm and 0.20 cm in the x and y directions, respectively, and a thickness of 4 cm. In this study, two phantoms with different structures, including simple cardiac phantom and Nonuniform Rational B-spline CArdiac-Torso (NCAT) phantom, were used to evaluate the performance of scatter correction methods in imaging with ^{99m}Tc and ^{201}Tl radioisotopes. In the simulations related to the simple cardiac phantom and the NCAT phantom, the distance from the coordinate origin to the detector surface was equal to 20 and 30 cm, respectively. The base activity used in the simulation of both phantoms was 370 MBq. 64 projections are acquired by rotating the camera 360° and 180° in simulating the simple cardiac phantom and the NCAT phantom, respectively. In the final stage, MATLAB software was used to reconstruct the images and evaluate the scatter correction methods. In this study, the simulations were repeated 5 times for each phantom, and finally, the mean values of obtained data were used to evaluate the correction methods.

Scatter correction methods and energy window settings

Dual-energy window method

In this method,[8] a secondary window located in the Compton area of the energy spectrum of the investigated radioisotope, known as the "Compton window," was used for scatter correction. The essential assumption in this method is that the spatial distribution of the counts acquired in Compton window (T_C) is the same as the spatial distribution of the scatter counts in the main window (S_{pk}), and that only quantitatively, they differ in a factor k:

$$S_{pk}(i,j) = kT_C(i,j) \quad (1)$$

where, (i, j) denotes the location of a given pixel in the image matrix.

In this study, the method proposed by reference [12] was used to calculate the k-value. In this method, equation (1) was replaced by the following linear fitting equation:

$$S_{pk}(i,j) = aT_C(i,j) + b \quad (2)$$

where, a and b are the coefficients of the linear fitting equation. These coefficients were obtained for an arbitrary number of projections (17 projections for both the simple cardiac phantom and the NCAT phantom). Finally, equation (2) with mean coefficients a and b was directly used instead of equation (1).

Triple-energy window method with trapezoidal approximation

In this correction method,[12] two narrow windows centered on both sides of the main window were used to estimate the scatter counts of the main window. In this approximation, the area under the scatter spectrum of the main window was estimated using the area of a trapezoid. The two heights of this trapezoid were calculated by dividing the total counts of the two narrow windows by their width:

$$S_{pk}(i,j) = \left[\frac{T_{low}(i,j)}{w_{low}} + \frac{T_{up}(i,j)}{w_{up}}\right]\frac{w_{pk}}{2} \quad (3)$$

where $T_{low}(i, j)$ and $T_{up}(i, j)$ are the pixel counts of the projections related to the lower and upper narrow windows,

respectively. Furthermore, w_{low} and w_{up} were the widths of these two narrow windows. The widths of the lower and upper narrow windows were chosen so that the ratio of the total counts of these two windows to their width was approximately equal to the scatter counts in the lower and upper energy limits of the main window respectively.

Energy window settings for scatter correction

Tc-99m radioisotope has a photopeak at 140 keV and Tl-201 radioisotope has three photopeaks at 68 keV, 135 keV, and 168 keV. Hence, for Tc-99m, a 20% window centered at 140 keV, and for Tl-201, as suggested by reference [4] a 30% window centered at 75 keV (instead of the usual photopeak energy of 68 keV) and two 20% windows centered at 135 keV and 168 keV were used as the main windows.

In the case of Tc-99m radioisotope, a 30% Compton window centered at 109 keV was used for the DEW correction method. In addition, an 8% lower narrow window centered at 121 keV and a 6% upper narrow window centered at 159 keV were used for the TEW correction method. Figure 1 illustrates the location of the energy windows used for scatter correction of the images obtained from Tc-99m radioisotope.

In the case of Tl-201 radioisotope, the contribution of scatter counts included in the first main window was much more than the other two main windows. Therefore, the scatter correction for this radioisotope was limited to the correction for the first main window. Finally, after applying the corrections on the projections obtained from the first main window, the projections of the other two main windows were added to the corrected projections of the first main window. Accordingly, in the case of Tl-201, a 34% window centered at 51 keV was used as Compton window for the DEW correction method. Furthermore, two 8% and 6% windows centered at 56 keV and 92 keV were used as lower and upper narrow windows, respectively, for the TEW correction method. Figure 2 illustrates the location of the energy windows used for scatter correction of the images obtained from Tl-201 radioisotope.

Phantoms and assessment criteria

Simple cardiac phantom

In the first step, a simple cardiac phantom was used to evaluate the performance of the scatter correction methods in imaging with ^{99m}Tc and ^{201}Tl radioisotopes. This phantom is a combination of a half-spherical shell and a cylindrical shell,

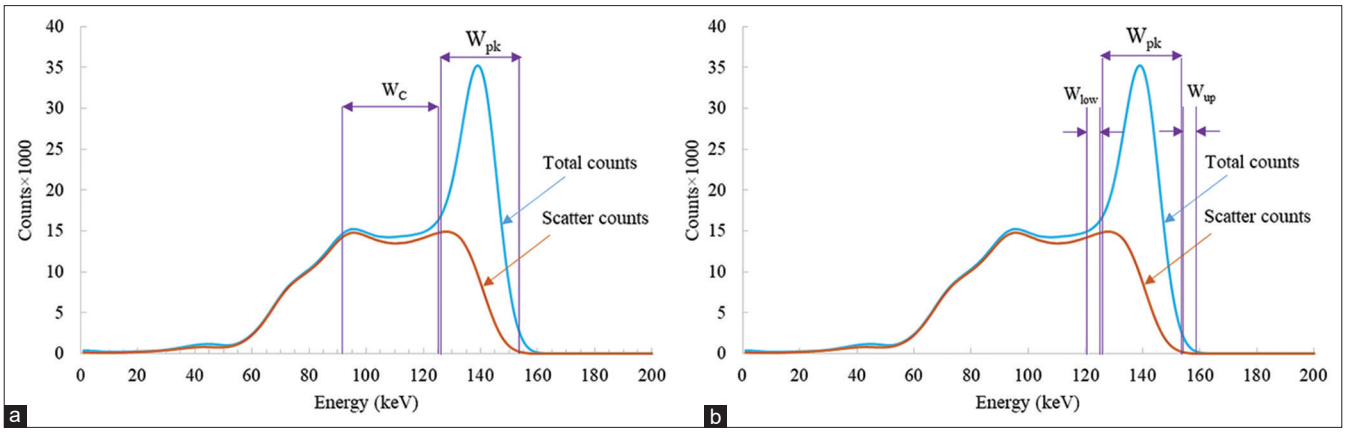

Figure 1: Illustration of the energy window settings used for, (a) Dual-energy window and, (b) Triple-energy window correction methods in the ^{99m}Tc energy spectrum from a typical simulation

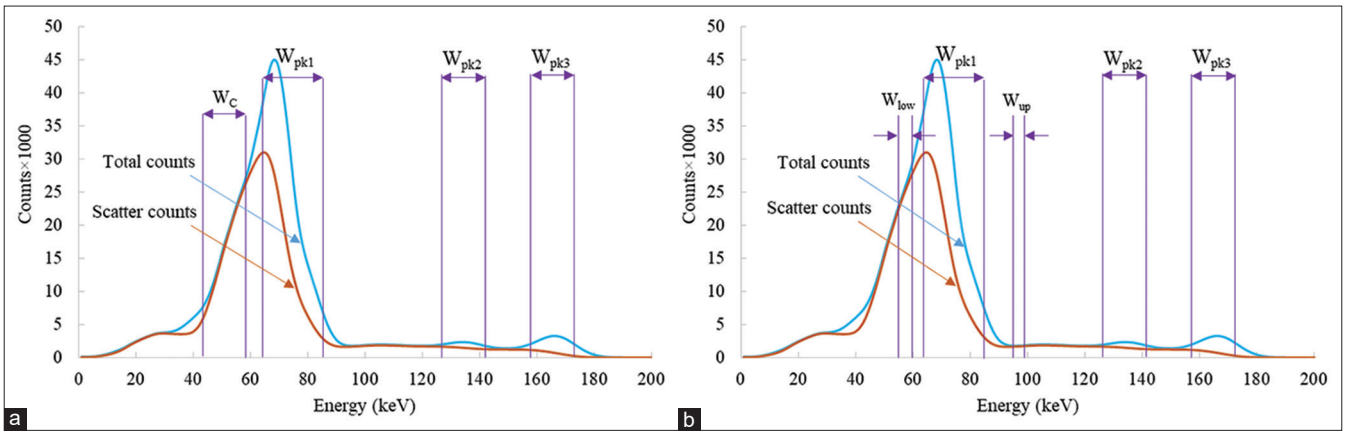

Figure 2: Illustration of the energy window settings used for, (a) Dual-energy window and, (b) Triple-energy window correction methods in the ^{201}Tl energy spectrum from a typical simulation

both with the same thickness of 1 cm. A view of this phantom together with a projection and a slice of a reconstructed image of this phantom are shown in Figure 3.

NCAT phantom

In the next step, the NCAT phantom was used to more accurately evaluate the performance of the scatter correction methods. This phantom provides a realistic model of the human anatomy. Figure 4 shows two views of this phantom together with an arbitrary projection obtained from this phantom. Since the organ investigated in this study was the heart, by choosing the appropriate image pixel size in the simulation of this phantom, only the area limited to the heart was investigated.

Image contrast

In the case of both phantoms, the assessment criterion used was the image contrast, calculated using a linear profile passing through an arbitrary slice of the reconstructed image of these phantoms. A sample of this linear profile, obtained from a simulation of the simple cardiac phantom, is shown in Figure 5. From the figure, the image contrast is defined as follows:[4]

$$C = \frac{MC_{AB} - C_C}{MC_{AB} + C_C} \quad (4)$$

where MC_{AB} indicates the mean counts at the two maximum points A and B, and C_C indicates the counts at the minimum point C between these two peaks.

Results

The dual-energy window correction method

To apply the DEW correction method, it is necessary to first determine the mean coefficients a and b in equation (2). A sample of linear fitting of the scatter counts of the main window with the total counts of the Compton window for an arbitrary projection is shown in Figure 6. Furthermore, the summary of the results obtained from 5 simulation tests is given in Table 1. From the data of this table, the mean values of fitting coefficients a and b obtained from 5 simulation tests, performed for each of the two investigated phantoms with ^{99m}Tc and ^{201}Tl radioisotopes, are as follows:

for simple cardiac phantom

$$\begin{cases} {}^{99m}Tc \rightarrow S_{pk}(i,j) = 0.7575\, T_C(i,j) - 0.4876 \\ {}^{201}Tl \rightarrow S_{pk}(i,j) = 1.328\, T_C(i,j) - 0.2345 \end{cases} \quad (5)$$

for NCAT phantom

$$\begin{cases} {}^{99m}Tc \rightarrow S_{pk}(i,j) = 0.5812\, T_C(i,j) - 0.1018 \\ {}^{201}Tl \rightarrow S_{pk}(i,j) = 1.178\, T_C(i,j) - 0.03423 \end{cases} \quad (6)$$

Therefore, in DEW method, instead of a constant k-value, the above relations were used for scatter correction of the images obtained from two investigated phantoms. According to relations 5 and 6, the value of coefficient a depends not only on the radioisotope used in imaging but also on the structure of the phantom used for evaluation. From the above relations, the value of this coefficient for ^{201}Tl radioisotope is greater than ^{99m}Tc radioisotope.

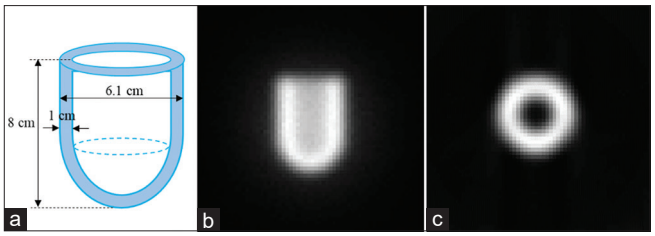

Figure 3: (a) A view of the simple cardiac phantom along with, (b) A projection and, (c) An arbitrary slice of the reconstructed images from this phantom

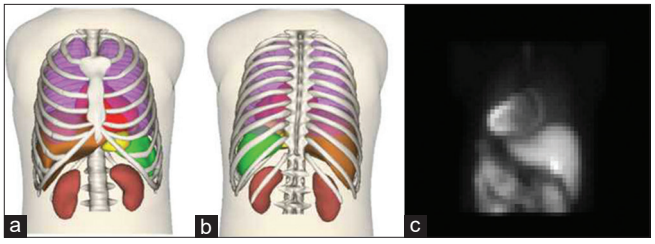

Figure 4: (a) Anterior and, (b) Posterior views of the NCAT phantom[13] along with, (c) An arbitrary projection from this phantom

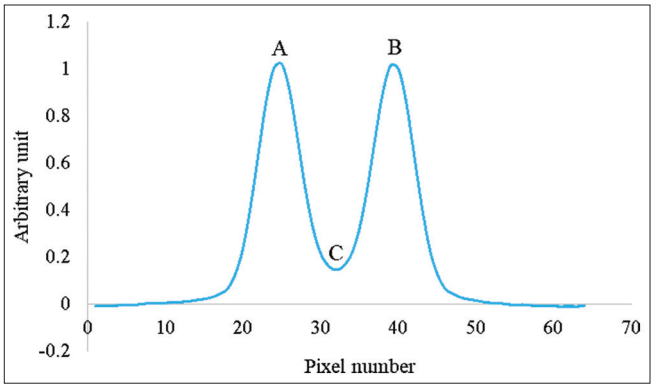

Figure 5: A sample of a linear profile passing through an arbitrary slice of the reconstructed image from the simple cardiac phantom

The triple-energy window correction method

Before investigating the results of the TEW correction method, first, using equation (3), we investigated the accuracy of this correction approximation in estimating the area under the scatter spectrum of the main window. Figure 7 shows the estimated trapezoidal area of this correction approximation in the energy spectra of ^{99m}Tc and ^{201}Tl radioisotopes.

According to the results obtained from the simulation of the simple cardiac phantom with ^{99m}Tc and ^{201}Tl radioisotopes, the scatter counts of the main window were equal to 227,000 and 338,000, and the scatter counts estimated from equation (3) were about 215,279 and 308,291, respectively, indicating the underestimations of about 5% and 8.7%. On the other hand,

the results obtained from the simulation of the NCAT phantom using ^{99m}Tc and ^{201}Tl radioisotopes show that the scatter counts of the main window were equal to 175,100 and 256,700, and the scatter counts estimated from equation (3) were about 169,947 and 244,441, respectively, indicating the underestimations of about 2.9% and 4.7%.

The image contrast

The image contrasts obtained from the simulation of the simple cardiac phantom and NCAT phantom using ^{99m}Tc and ^{201}Tl radioisotopes are given in Tables 2 and 3, respectively. According to the data of these two tables, it can be seen that in the case of both phantoms and both radioisotopes, the use of correction methods leads to an increase in image contrast compared to the situation before correction, and the amount of this increase for the DEW method is greater than that for the TEW method. In the case of the simple cardiac phantom, the relative increase of the mean image contrast obtained from the DEW and TEW correction methods is about 23.88% and

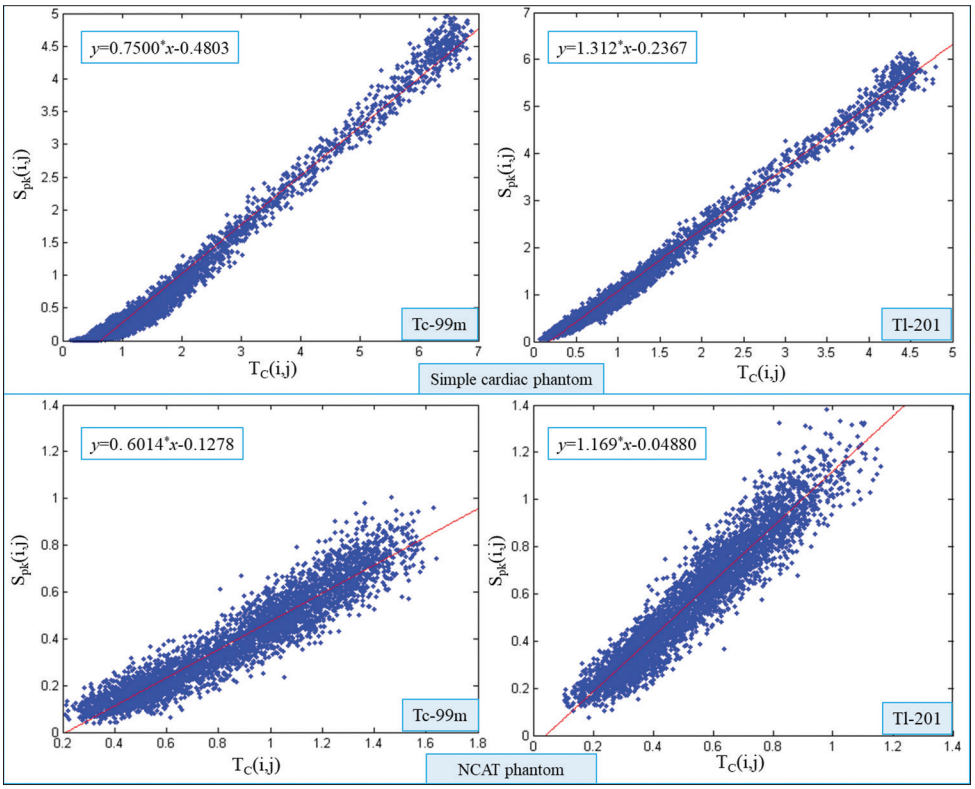

Figure 6: A sample of linear fitting of the pixel counts of an arbitrary scatter projection from the main window with the pixel counts of a corresponding projection from the Compton window related to the simple cardiac phantom (first row) and the NCAT phantom (second row) simulations using ^{99m}Tc and ^{201}Tl radioisotopes together with the equations of the fitting lines (the plotting of diagrams and the linear fitting of data was performed by MATLAB program). NCAT: Nonuniform Rational B-spline CArdiac-Torso

Table 1: Summary of results obtained for the mean fitting coefficients *a* and *b* from 5 simulation tests performed for the simple cardiac phantom and the NCAT phantom with ^{99m}Tc and ^{201}Tl radioisotopes

Test number	Simple cardiac phantom				NCAT phantom			
	Tc-99m		Tl-201		Tc-99m		Tl-201	
	a	*b*	*a*	*b*	*a*	*b*	*a*	*b*
1	0.7580 (0.001606)	−0.4881 (0.001873)	1.3281 (0.002606)	−0.2347 (0.002532)	0.5816 (0.02352)	−0.1023 (0.03955)	1.1761 (0.02056)	−0.03359 (0.03303)
2	0.7576 (0.001524)	−0.4882 (0.002735)	1.3271 (0.002645)	−0.2338 (0.002552)	0.5801 (0.02509)	−0.1005 (0.03999)	1.1797 (0.02135)	−0.03523 (0.03155)
3	0.7574 (0.001511)	−0.4874 (0.002417)	1.3279 (0.003160)	−0.2349 (0.002908)	0.5815 (0.02365)	−0.1019 (0.03973)	1.1777 (0.01847)	−0.03388 (0.03186)
4	0.7574 (0.001147)	−0.4875 (0.001934)	1.3275 (0.001981)	−0.2343 (0.001948)	0.5819 (0.02491)	−0.1028 (0.04118)	1.1782 (0.02045)	−0.03419 (0.03285)
5	0.7571 (0.001388)	−0.4869 (0.001953)	1.3277 (0.002785)	−0.2350 (0.002667)	0.5810 (0.02426)	−0.1017 (0.03965)	1.1780 (0.02157)	−0.03428 (0.03243)

The values in parentheses are SDs. SD: Standard deviation, NCAT: Nonuniform Rational B-spline CArdiac-Torso

Table 2: Image contrasts obtained from 5 simulation tests performed for the simple cardiac phantom by using ^{99m}Tc and ^{201}Tl radioisotopes, together with mean values and standard deviations

Radioisotope	Status	Test 1	Test 2	Test 3	Test 4	Test 5	Mean	SD
Tc-99m	DEW	0.9283	0.9317	0.9318	0.9321	0.9290	0.9306	0.001785
	TEW	0.8356	0.8450	0.8430	0.8467	0.8450	0.8431	0.004371
	NC	0.7492	0.7533	0.7512	0.7509	0.7513	0.7512	0.001458
	Primary	0.9595	0.9632	0.9633	0.9619	0.9635	0.9623	0.001677
Tl-201	DEW	0.8527	0.8424	0.8527	0.8373	0.8486	0.8467	0.006754
	TEW	0.7968	0.793	0.7978	0.7895	0.7875	0.7929	0.004471
	NC	0.6574	0.6559	0.6578	0.6514	0.6544	0.6554	0.002598
	Primary	0.9419	0.9351	0.9395	0.9365	0.9368	0.9380	0.002718

DEW: Dual-energy window, TEW: Triple-energy window, NC: Noncorrection, SD: Standard deviation

Table 3: Image contrasts obtained from 5 simulation tests performed for the NCAT phantom by using ^{99m}Tc and ^{201}Tl radioisotopes, together with mean values and standard deviations

Radioisotope	Status	Test 1	Test 2	Test 3	Test 4	Test 5	Mean	SD
Tc-99m	DEW	1.045	0.9472	0.9762	1.054	0.9953	1.004	0.04543
	TEW	0.9977	0.9952	0.9469	1.0164	0.9388	0.9790	0.03412
	NC	0.8417	0.7995	0.8101	0.8469	0.8002	0.8197	0.02294
	Primary	1.047	1.015	1.035	1.030	1.022	1.030	0.01228
Tl-201	DEW	0.8681	0.9220	0.9104	0.8270	0.8719	0.8799	0.03776
	TEW	0.8450	0.8851	0.8966	0.8115	0.8578	0.8592	0.03372
	NC	0.7027	0.6962	0.7050	0.6576	0.6827	0.6888	0.0195
	Primary	0.9897	1.019	0.9767	0.9764	0.9616	0.9847	0.02161

DEW: Dual-energy window, TEW: Triple-energy window, NC: Noncorrection, SD: Standard deviation. NCAT: Nonuniform Rational B-spline CArdiac-Torso

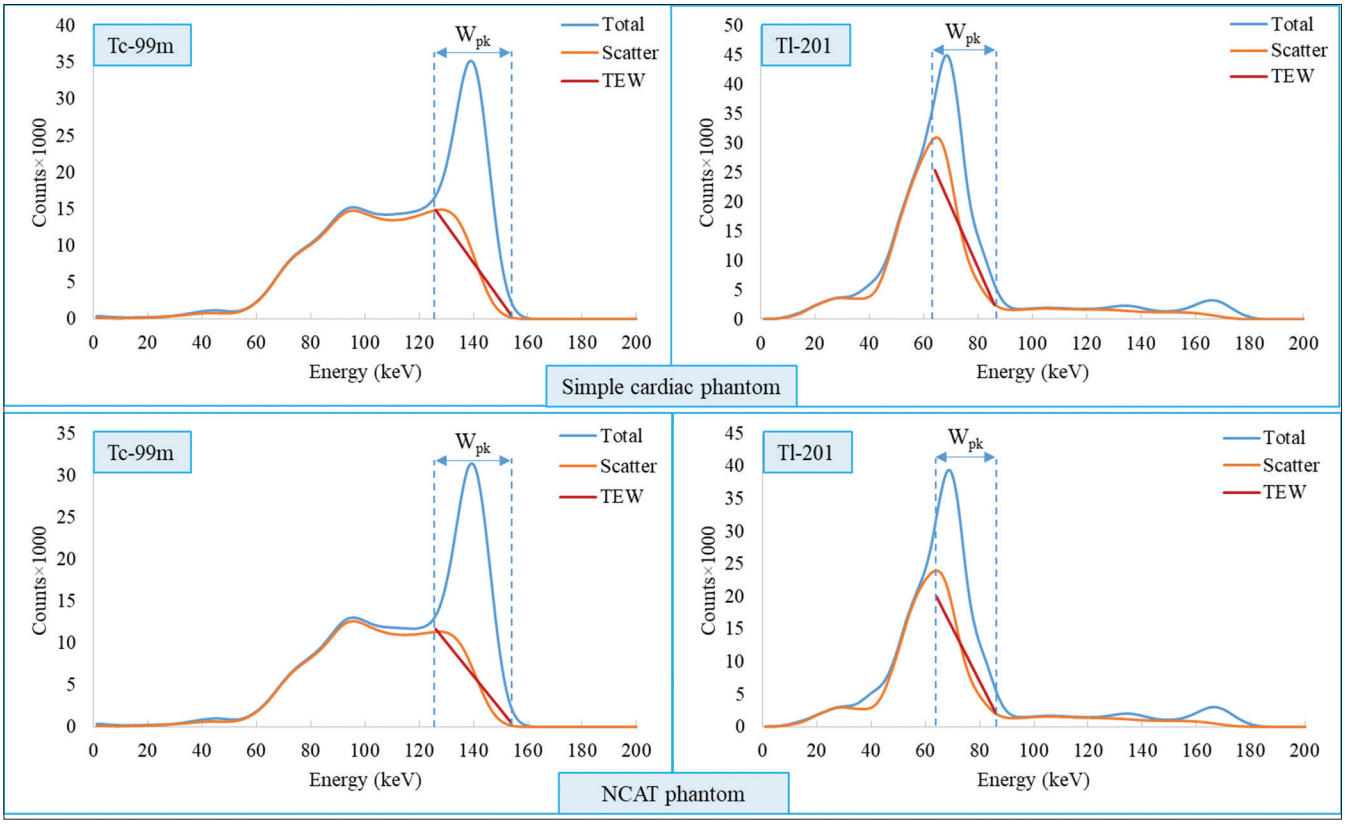

Figure 7: Energy spectra of total and scatter counts together with the scatter area estimated from the trapezoidal approximation for the simple cardiac phantom (first row) and the NCAT phantom (second row) simulations with ^{99m}Tc and ^{201}Tl radioisotopes. NCAT: Nonuniform Rational B-spline CArdiac-Torso

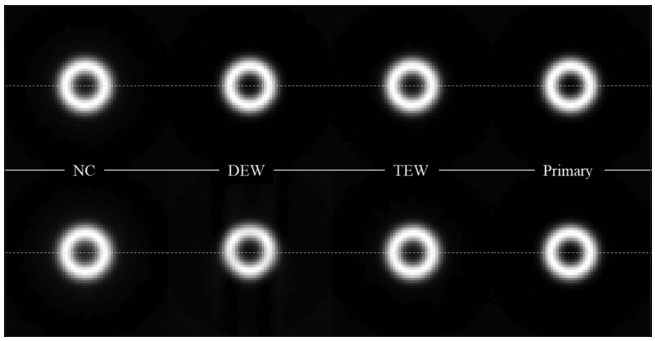

Figure 8: An arbitrary slice of reconstructed images from the simple cardiac phantom for ^{99m}Tc (first row) and ^{201}Tl (second row) radioisotopes in four situations: Noncorrection, corrected by DEW and TEW method along with the images obtained from the primary counts. NC: Noncorrection, DEW: Dual-energy window, TEW: Triple-energy window

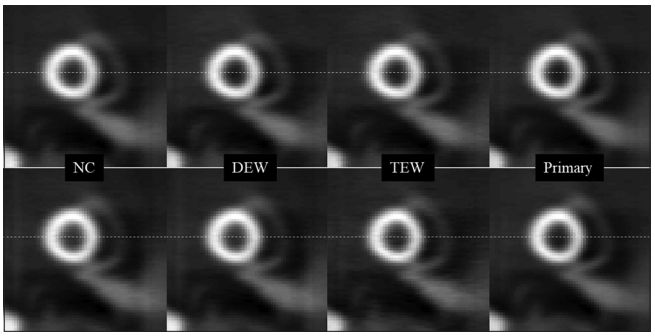

Figure 9: An arbitrary slice of reconstructed images from the NCAT phantom for ^{99m}Tc (first row) and ^{201}Tl (second row) radioisotopes in four situations: Noncorrection, corrected by dual-energy window and triple-energy window method along with the images obtained from the primary counts. NC: Noncorrection, DEW: Dual-energy window, TEW: Triple-energy window

12.23%, for ^{99m}Tc radioisotope, and about 29.19% and 20.98% for ^{201}Tl radioisotope, respectively. On the other hand, in the case of the NCAT phantom, these relative increases are about 22.48% and 19.43%, for ^{99m}Tc radioisotope, and about 27.74% and 24.74% for ^{201}Tl radioisotope. From these results, in the case of both phantoms, the relative increase of contrast in images obtained from ^{201}Tl radioisotope is more than ^{99m}Tc images.

Figures 8 and 9 show an arbitrary slice of the reconstructed image of the simple cardiac phantom and the NCAT phantom, respectively, in four situations: noncorrection, corrected by DEW and TEW methods, together with the images obtained from the primary counts in simulation using ^{99m}Tc and ^{201}Tl radioisotopes. From these figures, it is clear that the use of correction methods leads to the improvement of the image contrast. In addition, the linear profiles corresponding to each of these images are shown in Figure 10. From this figure, in the case of Tc-99m radioisotope, the DEW-corrected profiles have a better agreement with the primary profiles than the TEW corrected profiles. In the case of Tl-201 radioisotope, the DEW and TEW corrected profiles are higher than the primary profiles, indicating an underestimation of the scatter counts of the main window by both these correction methods. On the other hand, in the case of both radioisotopes, the DEW and TEW corrected profiles for the NCAT phantom are closer to each other than those for the simple cardiac phantom, indicating an almost same estimation of the scatter counts of the main window by both correction methods.

Discussion and Conclusion

This study aims to compare the performance of scatter correction methods in improving the quality of images obtained from cardiac SPECT imaging with Tc-99m and Tl-201 radioisotopes. Since these two radioisotopes are widely used in cardiac SPECT imaging, investigation of the quality of images obtained from these radioisotopes before and after applying the correction methods can provide useful information for researchers. In the present study, two scatter correction methods, DEW method and TEW method with trapezoidal approximation, with energy window settings applicable in clinical systems are evaluated.

In this study, SIMIND Monte Carlo simulation is used to evaluate the scatter correction methods in imaging with Tc-99m and Tl-201 radioisotopes. For more accurate evaluation, two phantoms with different structures, including the simple cardiac phantom and the NCAT phantom, are used. In the implementation of DEW correction method, instead of using a constant *k*-value, the linear fitting method is used to improve this correction method. The linear fitting of data and calculating the fitting coefficients *a* and *b* is performed in MATLAB program. This program is also used to reconstruct the images and calculate the image contrast values. To obtain more accurate and valid results, the simulations are repeated 5 times for each phantom, and finally, the mean values of the image contrasts obtained from these 5 tests together with the standard deviations are used for the analysis of the results.

The results obtained from the simulations show that in the case of both phantoms, the use of scatter correction methods leads to an improvement in the contrast of the images obtained from both radioisotopes. Furthermore, according to the obtained results, in the case of both radioisotopes, the degree of improvement in contrast for the images corrected by the DEW method is more than the images corrected by the TEW method. In addition, although the initial contrast of Tl-201 images was lower compared to Tc-99m images, the relative increase of contrast after implementing the correction methods was more significant for Tl-201.

Another point, according to the results obtained from this study is that in the case of the both investigated phantoms, the TEW correction method for the Tc-99m radioisotope provides a better estimation of the scatter counts of the main window than for the Tl-201 radioisotope. The reason for this is the difference in the shape of the spectra of these two radioisotopes. In fact, from Figures 1 and 2, it is clear that the lower narrow window for Tc-99m radioisotope can

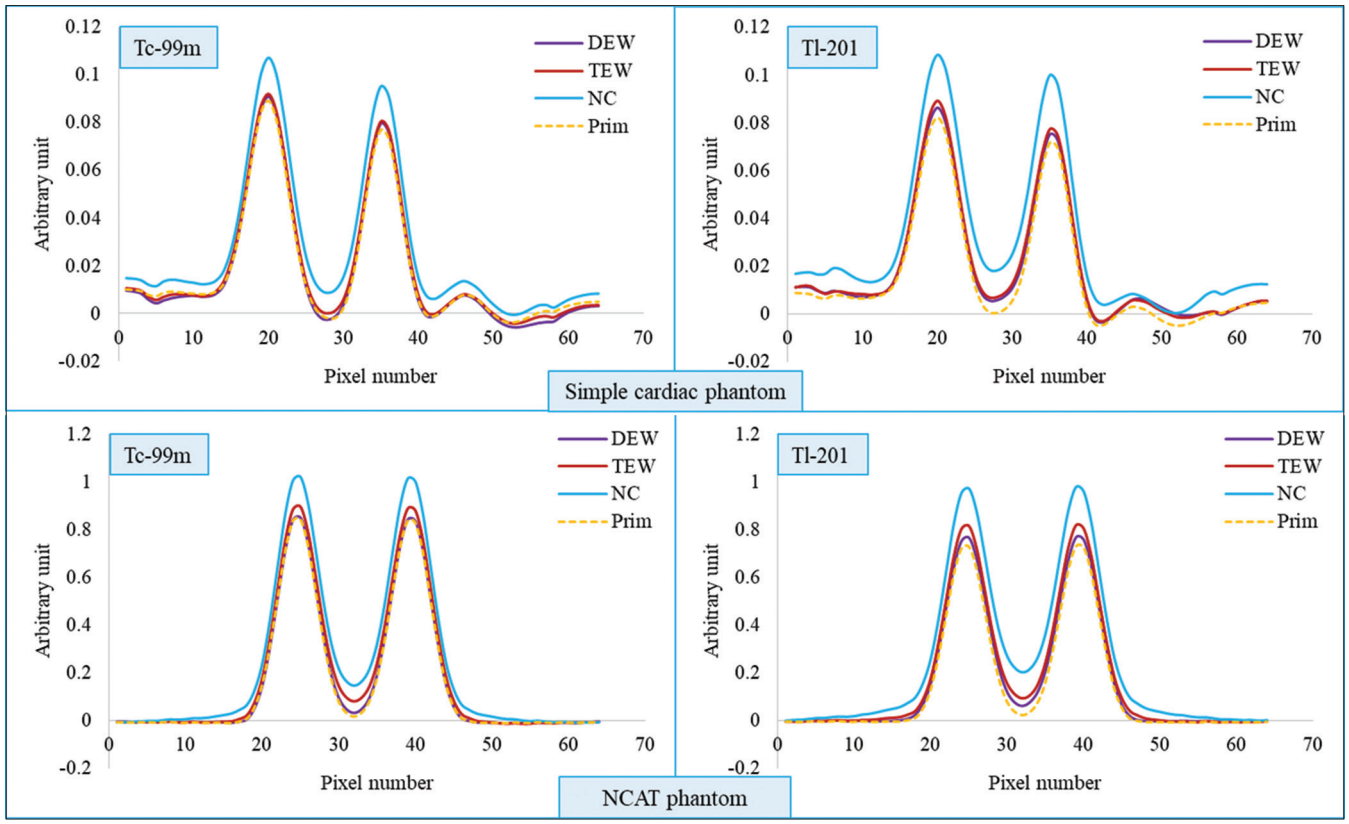

Figure 10: Linear profiles corresponding to the lines marked in Figures 8 and 9 for the simple cardiac phantom (first row) and the NCAT phantom (second row) simulations with ^{99m}Tc and ^{201}Tl radioisotopes. NC: Noncorrection, DEW: Dual-energy window, TEW: Triple-energy window, NCAT: Nonuniform Rational B-spline CArdiac-Torso

provide a more accurate estimate of the scatter counts of the lower energy limit of the main window than for Tl-201 radioisotope. However, in the case of both radioisotopes, using the trapezoidal approximation leads to an underestimation of the scatter counts of the main window. Although this underestimation leads to a less-than-ideal scatter correction for the images obtained from both radioisotopes, it nevertheless results in a significant reduction of the contribution of scatter counts included in the main window and therefore, a significant improvement in the image contrast.

On the other hand, the value of the fitting coefficient a in the equation (2) is different depending on the structure of the phantom under investigation, and so, contrary to popular belief, using a constant k-value (typically a value of 0.5) in the DEW correction method to different structures can lead to large errors.

One of the limitations of the correction methods investigated in this research is their dependence on the energy spectrum of the used radioisotope. Furthermore, the obtained energy spectrum depends on the structure of the scattering medium under investigation (phantom or patient). By changing the structure of the scattering medium, the spectrum of the considered radioisotope has changed to some extent. One of the consequences of this problem is that the optimized energy window settings for the scatter correction of images obtained from one structure may be not optimal for another structure. In addition, in the present study, the motion of the heart, which can cause additional complications in the energy spectrum, is not taken into account. Investigating these effects require more studies.

Financial support and sponsorship

Nil.

Conflicts of interest

There are no conflicts of interest.

References

1. Gibbons RJ. Myocardial perfusion imaging. Heart 2000;83:355-60.
2. Pagnanelli RA, Basso DA. Myocardial perfusion imaging with 201Tl. J Nucl Med Technol 2010;38:1-3.
3. Kalantari F, Rajabi H, Yaghoobi N. Optimized energy window configuration for 201Tl imaging. J Nucl Med Technol 2008;36:36-43.
4. Noori-Asl M, Hosseinifar H. Reduction of contribution of scattered photons by optimization of energy window settings in 201Tl spect imaging: A simulation study. J Instrum 2022;17:P08017.
5. Kojima A, Takaki A, Noguchi T, Matsumoto M, Katsuda N, Tomiguchi S, *et al.* Optimum energy window setting on Hg-201 x-rays photopeak for effective Tl-201 imaging. Ann Nucl Med 2005;19:541-7.
6. Baggish AL, Boucher CA. Radiopharmaceutical agents for myocardial perfusion imaging. Circulation 2008;118:1668-74.
7. Radioisotopes in Medicine, World Nuclear Association; 2023. Available from: https://world-nuclear.org/information-library/non-power-nuclear-applications/radioisotopes-research/radioisotopes-in-medicine.aspx. [Last accessed on 2024 Apr 20]

8. Noori-Asl M, Sadremomtaz A, Bitarafan-Rajabi A. Evaluation of six scatter correction methods based on spectral analysis in (99m) Tc SPECT imaging using SIMIND Monte Carlo simulation. J Med Phys 2013;38:189-97.
9. Ljungberg M, Strand SE. A Monte Carlo program simulating scintillation camera imaging. Comput Methods Programs Biomed 1989;29:257-72.
10. Noori-Asl M, Bitarafan-Rajabi A. Simulation and patient studies of scatter correction in cardiac spect imaging. Iran J Med Phys 2019;16:430-8.
11. Noori-Asl M, Jeddi-Dashghapou S. Investigation of different components of parallel-hole collimator response to different radioisotope energies used in nuclear medicine imaging. J Med Phys 2022;47:294-300.
12. Noori-Asl M, Sadremomtaz A, Bitarafan-Rajabi A. Evaluation of three scatter correction methods based on estimation of photopeak scatter spectrum in SPECT imaging: A simulation study. Phys Med 2014;30:947-53.
13. Segars WP, Tsui BM. Study of the efficacy of respiratory gating in myocardial SPECT using the new 4D NCAT phantom. IEEE Trans Nucl Sci 2002;49:675-9.